Ferroelectric order in the chiral coordination polymers [Ln2(L*)2(ox)2(H2O)2] with Ln = Gd3+ or Dy3+, L* = ((S, S)-1,3-bis(1-carboxylethyl)imidazolium and ox = oxalate

Pierre Farger, Cedric Leuvrey, Marc Lenertz, Gregory Taupier, Kokou Dodzi Dorkenoo, Dris Ihiawakrim, Salia Cherifi-Hertel, Guillaume Rogez, Pierre Rabu, Emilie Delahaye

Journal of Inorganic and General Chemistry

ZAAC

Zeitschrift für anorganische und allgemeine Chemie

Accepted Article

Title: Ferroelectric order in the chiral coordination polymers [Ln2(L*)2(ox)2(H2O)2] with Ln = Gd3+ or Dy3+, L* = ((S, S)-1,3-bis(1-carboxylethyl)imidazolium and ox = oxalate.

Authors: Pierre Rabu, Pierre Farger, Cedric Leuvrey, Marc Lenertz, Gregory Taupier, Kokou D Dorkenoo, Dris Ihiawakrim, Salia Cherifi-Hertel, Guillaume Rogez, and Emilie Delahaye

To be cited as: *Z. anorg. allg. Chem.* **2024**, e202400005

Link to VoR: https://doi.org/10.1002/zaac.202400005

WILEY VCH

www.zaac.wiley-vch.de

10.1002/zaac.202400005

WILEY-VCH

ARTICLE

Ferroelectric order in the chiral coordination polymers $[Ln_2(L^*)_2(ox)_2(H_2O)_2]$ with Ln = Gd^{3+} or Dy^{3+}, L* = ((S, S)-1,3-bis(1-carboxylethyl)imidazolium and ox = oxalate.

P. Farger, [a] C. Leuvrey, [a] M. Lenertz, [a] G. Taupier, [a, b] K. D. Dorkenoo, [a] D. Ihiawakrim, [a] S. Cherifi-Hertel, [a] G. Rogez, [a] P. Rabu, [a] E. Delahaye*[a,c]

Tribute to Prof. Antoine Maignan to celebrate his 60th birthday ((optional))

Abstract: We evidence the ferroelectricity of two isostructural magnetic coordination networks obtained from a chiral imidazolium dicarboxylate salt ((S, S)-1,3-bis(1-carboxylethyl)imidazolium or [HL*]) and Gd^{3+} or Dy^{3+} ions in presence of oxalic acid (H_2ox). The two compounds exhibit a chiral structure *P*1 and ferroelectric properties. The crystallographic study shows that the Dy based-compound is isostructural to the Gd analog. The non-centrosymmetry of the two samples was further checked by means of nonlinear optical spectroscopy. The room temperature ferroelectric character of the compounds has been investigated through by an original method derived, from that used for thin films, made possible by preparing the sample as thin slices of resin containing inclusions of the coordination compounds.

Introduction

Ferroelectric materials have been the subject of considerable interest for decades, due to their numerous applications as sensors, actuators, memories, with recent developments in the field of energy harvesting devices using magnetoelectric, photovoltaic or electromechanical effects.[1–8] Protypical compounds are niobiates or titanates derivatives as well as Pb(Zr,Ti)O_3 ceramics,[9–11] bismuth ferrite $BiFeO_3$,[4] bismuth oxide layered structure (Aurivillius phases)[12–14] to cite few examples. More recently, the hybrid layered perovskites derived from the A_2PbX_4 structure, have been particularly under focus for application in photovoltaics and optoelectronics.[3,15,16]
Magnetoelectric and multiferroic materials, especially combining a ferroelectric and a ferromagnetic order, are of special interest for both fundamental and technological points of view.[17,18] Coexistence of these two ferroic properties, with or without synergy, can lead to potential applications in information storage or spintronics.[19–21]
As described in the reference works above, multiferroic materials are mainly covered by inorganic compounds (as Cr_2O_3 or ABO_3 perovskite oxides or chalcogenides such as $AgCrS_2$) or some 2D hybrid structures. Fundamentally, stabilizing ferroelectricity and ferromagnetism in one phase is not straightforward.[17,22] In particular, the presence of unpaired d-electrons needed to stabilize ferromagnetism, generally inhibits hybridization with the orbitals of the surrounding oxygen anions, and hence the displacements of the cations necessary for the establishment of a ferroelectric order. Therefore, the number of systems combining the two properties remains relatively small. As an alternative, the elaboration of multiferroic systems based on hybrid approach has emerged these last years.[23–25] The majority of these multiferroic hybrid materials concerns the Metal-Organic Frameworks (MOF) category, although some examples based on other molecule-based materials have been also reported.[26–30] Kobayashi reported the first example of multiferroic MOF in 2006.[31] This MOF is constituted of formate ligands connected to Mn^{2+} ions. It contains movable polar solvent molecules within porous cavities and exhibits ferrimagnetic and ferroelectric properties. These properties arise from the Mn^{2+} networks for the ferrimagnetism and from the ordering of the polar guest solvent molecules for the ferroelectricity. However, the relatively easy removability of the solvent molecules leads to a loss of the ferroelectric properties. Series of multiferroic MOFs were then reported involving non-volatile guest,[32] with an ABX_3 perovskite type structure where A holds for quaternary ammonium cations, B divalent transition metals and X formate ligands. In this family of MOFs, a paraelectric to (anti)ferroelectric transition is observed between 100 K and 150 K and is associated to a disorder-order transition of the H bonds established between the ammonium cations and the network.[33–37] Next to these MOFs exhibiting ferroelectricity mostly at low temperature, the development of MOFs showing ferroelectricity at room temperature and above has emerged with the use of chiral or flexible organic ligands to favour the crystallization in a polar point group.[38–40] However, the mechanisms responsible for multiferroicity in these MOFs and protocols for characterizing these properties are still under discussion.[41] In this context, we continue to investigate the properties of series of chiral imidazolium based transition metal or rare earth coordination networks.[42–45] This investigation has allowed the synthesis of the $[Gd_2(L^*)_2(ox)_2(H_2O)_2]$ compound using the chiral imidazolium salt named (S, S)-1,3-bis(1-carboxyethyl)imidazolium (noted hereafter [HL*]) with oxalate

[a] Dr P. Farger, [a] C. Leuvrey, [a] Dr M. Lenertz, [a] G. Taupier, [a, b] Prof K. D. Dorkenoo, [a] Dr D. Ihiawakrim, [a] Dr S. Cherifi-Hertel, [a] Dr G. Rogez, [a] Dr P. Rabu,* [a] Dr E. Delahaye*[a,c]
Institut de Physique et Chimie des Matériaux de Strasbourg, UMR 7504
Université de Strasbourg, CNRS
23 rue du Loess 67034 Strasbourg, France
E-mail: emilie.delahaye@lcc-toulouse.fr, pierre.rabu@ipcms.unistra.fr
[b] G. Taupier
Synthèse Caractérisation ANalyse de la MATière (ScanMAT) - UAR CNRS 2025
CNRS
Université de Rennes 1, Beaulieu - Bâtiment 10A, 263 avenue du Général Leclerc, 35042 Rennes, France
[c] Dr E. Delahaye
Laboratoire de Chimie de Coordination
CNRS, Université de Toulouse, UPS, INPT
205 route de Narbonne, 31077 Toulouse, France

Supporting information for this article is given via a link at the end of the document ((Please delete this text if not appropriate))

(noted hereafter ox) and Gd^{3+} ions and the possibility to consider this compound as possible alternative to qubits in quantum information science.[46,47]

In this paper, we report the synthesis of the Dy-based analogue and we investigate the ferroic properties of $[Gd_2(L^*)_2(ox)_2(H_2O)_2]$ and $[Dy_2(L^*)_2(ox)_2(H_2O)_2]$ compounds. The crystallographic studies show that the two networks are isostructural and crystallize in the triclinic polar space group P1. The observation of a second-harmonic generation ascertains the non-centrosymmetry of the compounds, motivating thus the investigations of their ferroelectricity. To overcome the lack of large crystals, ferroelectric measurements have been conducted on thin resin slices containing inclusions of the coordination compounds. These thin films are deposited between two copper electrodes through which the voltage is applied for both I(V) and C(V) measurements. A clear voltage-induced switching, characteristic of a ferroelectric order, was observed. In addition, magnetic measurements are consistent with antiferromagnetic interactions between the spin carriers in both compounds.

Results and Discussion

Synthesis

$[Gd_2(L^*)_2(ox)_2(H_2O)_2]$ and **$[Dy_2(L^*)_2(ox)_2(H_2O)_2]$** were synthesized in solvothermal conditions by reacting the imidazolium salt **$[HL^*]$** with $Gd(NO_3)_3$ or $Dy(NO_3)_3$ in presence of oxalic acid in a water/ethanol solution at 120°C for 3 days. After cooling to room temperature, colorless and entangled crystals were obtained with an average size of 100*50*20 μm^3 (Figure S1). Different synthesis conditions were explored. Although previous works on similar compounds reported that oxalic acid could form *in situ*, it was necessary in the present case to add oxalic acid in order to obtain crystalline solid. It was also observed that the title compounds could form only in presence of water in the reaction mixture.

Structural description and stability of $[Gd_2(L^*)_2(ox)_2(H_2O)_2]$ and $[Dy_2(L^*)_2(ox)_2(H_2O)_2]$

The single crystal structure of **$[Gd_2(L^*)_2(ox)_2(H_2O)_2]$** has been already published and was solved in the acentric triclinic space group *P*1, despite the disorder on the $[L^-]$ ligand.[46]

The asymmetric unit contains thus two Gd^{3+} ions, two $[L^{*-}]$ ligands, two oxalate ligands and two coordinated water molecules. The oxalate ligands are coordinated to two inequivalent Gd^{3+} ions giving rise to corrugated chains, themselves linked through imidazolium ligands, forming thus a three-dimensional network (Figure 1 and Figure S2).

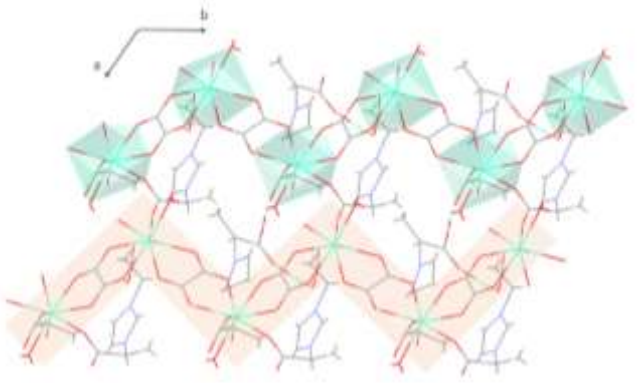

Figure 1. Representation of the connection between the imidazolium ligands and the undulating chains (in orange) constituted by oxalate ligands and Gd^{3+} ions in the 3D network **$[Gd_2(L^*)_2(ox)_2(H_2O)_2]$** (Gd in green, C in grey, O in red, N in blue). Coordination sphere for Gd^{3+} are shown in green. See CIF file in CCDC 2160787.[46]

Concerning the **$[Dy_2(L^*)_2(ox)_2(H_2O)_2]$** compound, single crystal X-ray analysis led to a structural model similar to that of the Gd analogue but with a higher disorder that could not be solved. Yet, the Rietveld refinement with the same structure on the powder X-ray diffraction patterns demonstrates that these two compounds are isostructural and fits well with the one calculated from the single crystal structure of **$[Gd_2(L^*)_2(ox)_2(H_2O)_2]$** (Figures 2 and S3).

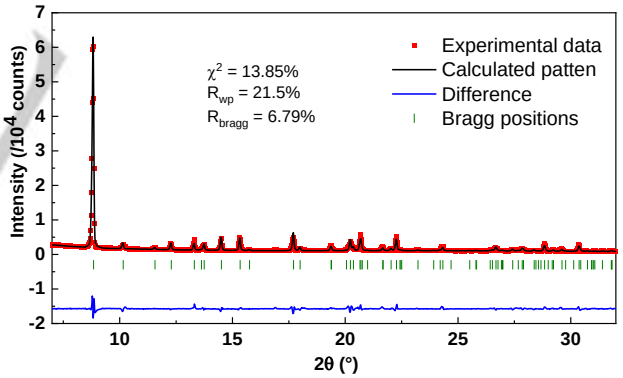

Figure 2. Results of the Rietveld refinement for the **$[Dy_2(L^*)_2(ox)_2(H_2O)_2]$** compound. The refined cell parameters at room temperature are a = 8.282(1) Å, b = 9.376(1) Å, c = 10.088(1) Å, α = 88.91(1)°, β = 83.58(1)°, γ = 68.54(1)°. Strong preferential orientation along [001] direction has been taken into account with the March function.

Thermo-gravimetric analysis of the two compounds indicates they are fairly stable up to 230° C, where a first weight loss is observed, corresponding to the removal of the coordinated water molecules (Figure S4). They decompose around 360° C with a complete weight loss at 900°C corresponding well to the formation of the oxides Gd_2O_3 or Dy_2O_3, respectively. The observed weight losses

10.1002/zaac.202400005

and the scheme of decomposition are in keeping with the formula confirming the purity of the compounds.
In addition to the thermo-gravimetric analysis, we followed the thermal evolution of the Dy analog by means of temperature solved X-ray diffraction to detect any structural phase transition before decomposition (Figure S5). The results indicate no structural change up to 230°C when it starts to decompose, forming an intermediate (unidentified) phase at 250°C before formation of the sesquioxide identified as the final product at 900°C.

Noncentrosymmetry of $[Gd_2(L^*)_2(ox)_2(H_2O)_2]$ and $[Dy_2(L^*)_2(ox)_2(H_2O)_2]$

The polarity of the space group was further investigated by means of second-harmonic generation (SHG). As shown in Figure 3, both **$[Gd_2(L^*)_2(ox)_2(H_2O)_2]$** and **$[Dy_2(L^*)_2(ox)_2(H_2O)_2]$** exhibit a frequency doubling process that is characteristic of non-centrosymmetric compounds. This observation of SHG in these compounds supports the space-group attribution made for the structure resolution and indicates that the two compounds are good candidates for ferroelectricity.

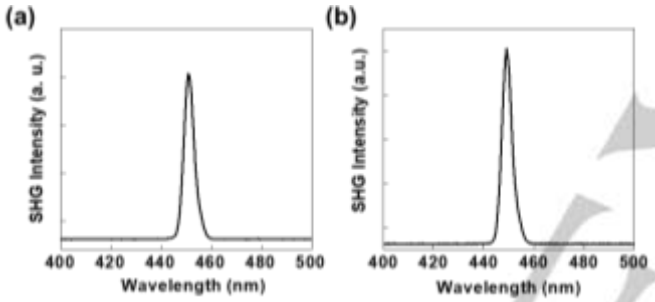

Figure 3. Second-harmonic generation signal at a fundamental wavelength λ_{exc} = 900 nm in compound **(a)** **$[Gd_2(L^*)_2(ox)_2(H_2O)_2]$** and **(b)** **$[Dy_2(L^*)_2(ox)_2(H_2O)_2]$**.

Ferroelectric measurements

The difficulty of probing and interpreting ferroelectric order has been pointed out in the literature.[41] This difficulty is mainly due to the high leakage current, which makes it difficult to detect electrical switching, and due to the small sample size and shape. Ferroelectric measurements are generally done on polycrystalline powder pellets either contacted with silver paste or with deposited metallic electrodes, or directly on single crystal contacted with metallic needles if the crystal size is sufficient. Yet, the indication of size/thickness and type of sample, as well as the frequency and voltage of measurement are often missing in the literature. Moreover, little attention is paid to electrochemical effects ensuring the stability of the compounds (*e. g.* loss of solvent molecules) during the dielectric measurements.
In the present work, these measurements have been realized on slices of resin incorporating **$[Gd_2(L^*)_2(ox)_2(H_2O)_2]$** inclusions of about 1 μm of thickness and contacted between two copper electrodes. Actually, the effective thickness of the composite sample was difficult to measure accurately. This setup has been used for three main reasons: (i) the size of the crystals was not sufficiently large to enable to address electrically one single crystal, (ii) to avoid the use of silver paste contacts since this method can lead to leakage current and interdiffusion with the material and (iii) because the use of sufficiently thin material slices allows to apply a rather low voltage to align the polarization in the field direction. It is important to note that after embedding in resin the **$[Gd_2(L^*)_2(ox)_2(H_2O)_2]$** compound is not altered (Figure S6).
The measurement of the polarization as a function of the applied voltage (P(V)) on **$[Gd_2(L^*)_2(ox)_2(H_2O)_2]$** is shown in Figure S7 with comments. This P(V) curve shows a hysteresis loop with a rounded shape. This effect is characteristic of leaky samples as discussed by Scott.[20] The observation of such P(V) loops, although encouraging, is therefore not by itself a proof of the existence of a ferroelectric order. The ferroelectricity at fixed temperature is better demonstrated by the variation of the displacement current with the voltage (I(V) measurements) applied at high frequency values[48]) and by capacitance-voltage measurements (C(V)), given that both curves should exhibit characteristic polarization switching peaks. These measurements have been realized on **$[Gd_2(L^*)_2(ox)_2(H_2O)_2]$** and are reported in Figure 4. The presence of two peaks in the I(V) curve at high frequency (marked by vertical marks in Figure 4a) indicate the existence of a switching current typically observed in ferroelectric materials. Moreover, the observation of typical butterfly-type C(V) loop (figure 4b) further allows to ascertain the existence of a ferroelectric switching in **$[Gd_2(L^*)_2(ox)_2(H_2O)_2]$** compound.
The same butterfly-like C(V) loop is also observed in the isostructural compound **$[Dy_2(L^*)_2(ox)_2(H_2O)_2]$** (Figure S7), underlining the generality of this approach.

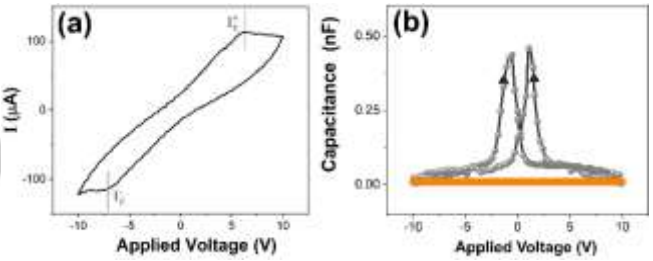

Figure 4. (a) I(V) curve measured at a voltage sweep frequency of 1 kHz and **(b)** C(V) static capacitance response to a DC bias voltage superposed to a small excitation voltage (1-2 V at 200 Hz) in non-centrosymmetric **$[Gd_2(L^*)_2(ox)_2(H_2O)_2]$** (gray dots) and centrosymmetric **$[Gd(L_2)(ox)(H_2O)]$** (orange dots). The arrows in the C(V) curve indicate the direction of the applied voltage. Both measurements are conducted at room temperature.

C(V) measurements have been also realized on the resin alone and on slices of resin containing a network **$[Gd_2(L)_2(ox)(H_2O)]$** showing a composition similar to **$[Gd_2(L^*)_2(ox)_2(H_2O)_2]$** but crystallizing in a non-polar space group (see orange dots in Figure 4b). No signal is observable on these C(V) curves confirming that the ferroelectricity does not result from possible charges trapped between the resin and the crystals. The butterfly C(V) curves typically observed in ferroelectrics are thus attributed to the polar compound **$[Gd_2(L^*)_2(ox)_2(H_2O)_2]$**.

10.1002/zaac.202400005

Magnetic Properties

The magnetic properties of **$[Dy_2(L^*)_2(ox)_2(H_2O)_2]$** have been investigated in the 1.8 - 300 K under a 0.5 T magnetic field. The χT value for **$[Dy_2(L^*)_2(ox)_2(H_2O)_2]$** is 13.58 emu.K.mol^{-1} at 300 K and is in line with the theoretical value for one isolated Dy^{3+} ions (S = 5/2, L = 5, $^6H_{15/2}$, g = 4/3, $\chi_M T_{free\ ion}$ = 14.17 emu.K.mol^{-1}).[49] The χT product is nearly constant until 170 K and then decreases to 7.93 emu.K.mol^{-1} at 1.8 K (Figure 5). This behavior can be ascribed to the depopulation of the low lying states (m_J states) arising from the $^6H_{15/2}$ ground state splitted through the action of crystal-field (the ground state here is well below the first excited state $^6H_{13/2}$ which is not populated) and possible existence of small antiferromagnetic interaction just like in the Gd analogue.[46]

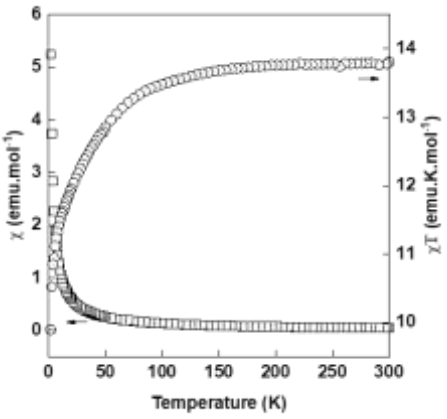

Figure 5. Plots of the magnetic susceptibility χ (open circles) and χT product (open squares) versus T for the compound **$[Dy_2(L^*)_2(ox)_2(H_2O)_2]$**.

A very good fit of the magnetic data has been obtained using the analytical expression for Dy^{3+} ions (given in SI), with the best refined value of the zero field splitting (ZFS) parameter Δ = 0.237(3) cm^{-1} (Figure S11). For the Gd analogue, the data could be analysed with appropriate analytical expression of the susceptibility for classical S = 5/2 chains of Gd^{3+} ions leading to the best refined values g = 2.12 and J = -0.009 cm^{-1} for the Landé factor and weak intrachain antiferromagnetic interaction.[46]

Conclusions

We report herein the ferroelectric behaviour of two magnetic networks based on a chiral imidazolium dicarboxylate salt and Gd^{3+} or Dy^{3+} ions in presence of oxalate ligand. In particular, the ferroelectricity is ascertained unambiguously by the measurements of C(V) curves following an unprecedented convenient protocol that can be generalized for the study of powder or microcrystalline hybrid networks. The present result offers new possibility for evidencing ferroelectricity in polycrystalline hybrid compounds of low robustness (both mechanical and thermal) and paves the way for the elaboration of new intrinsic multiferroic hybrid networks with versatile properties.

Experimental Section

Materials and general methods.

$Gd(NO_3)_3{\cdot}6H_2O$ and oxalic acid were purchased from Alfa Aesar and were used as received. Elemental analyses for C, H, N were carried out at the Service de Microanalyses of the Institut de Chimie de Strasbourg. NMR spectra in solution were recorded using a Bruker AVANCE 300 (300 MHz) spectrometer. The powder XRD patterns were collected with a Bruker D8 diffractometer (Cu Kα_1 = 1.540598 Å). Optical rotation was measured using an Anton Paar MCP-200 polarimeter (glass cells with optical path lengths of 10 cm and a total volume of 0.7 ml). The SEM images were obtained with a JEOL 6700F scanning electron microscope (SEM) equipped with a field emission gun (FEG), operating at 15 kV in the composition mode of the instrument. TGA-TDA experiments were performed using a TA instrument SDT Q600 (heating rates of 5°C·min^{-1} under air stream).

Synthesis of the (S, S)-1,3-bis(1-carboxyethyl)imidazolium ligand [HL*] and of $[Gd_2(L^*)_2(ox)_2(H_2O)_2]$

[HL*] and **$[Gd_2(L^*)_2(ox)_2(H_2O)_2]$** were synthesized according to previous published protocols.[50,51,46] Crystallographic data for **$[Gd_2(L^*)_2(ox)_2(H_2O)_2]$** can be found with the CCDC reference number 2160787.

Synthesis of $[Dy_2(L^*)_2(ox)_2(H_2O)_2]$

Same solvothermal procedure was used for the synthesis of **$[Dy_2(L^*)_2(ox)_2(H_2O)_2]$**. Typically, the imidazolium ligand [HL*] (0.50 mmol), $Dy(NO_3)_3.5H_2O$ (0.50 mmol) and oxalic acid H_2ox (0.25 mmol) are introduced in a water/ethanol mixture (1.5 mL, 1:1 vol) and heated in a 6 ml Teflon lined autoclave at 393 K for 3 days. The crystalline material was filtered and washed with ethanol (yield: 37 %).

Elemental analysis for **$[Dy_2(L^*)_2(ox)_2(H_2O)_2]$** (*M = 959.0 g.mol^{-1}*) Found (Calc.): C 26.70 (26.52), H 2.71 (2.71), N 5.49 (5.84). IR (reflectance, cm^{-1}): 3300 (w), 3134 (w) , 3095 (w), 1702 (w), 1599 (s), 1462 (w), 1400 (w), 1364 (w), 1313 (m), 1260 (w), 1175 (m), 1117 (w), 1081 (w), 1020 (w), 981 (w), 888 (w), 793 (s), 704 (w), 658 (w), 631 (w), 587 (w), 485 (m).

Synthesis of $[Gd(L_2)(ox)(H_2O)]$ using the ligand L_2^- = 1,3-bis(1-carboxylatomethyl)-1H-imidazol-3-ium ligand

$[Gd(L_2)(ox)(H_2O)]$ was synthesized as previously described by reacting in solvothermal conditions, $Gd(NO_3)_3.6H_2O$, [HL_2] and oxalic acid in water/ethanol mixture.[44] **$[Gd(L_2)(ox)(H_2O)]$** was found to crystallize in the centrosymmetric space group $P2_1/a$ (CCDC reference number 1541843).

Second Harmonic Generation (SHG) Measurements. SHG measurements were performed with an inverted microscope (Olympus IX71). The excitation beam at 900 nm, provided by a Ti:Sapphire laser (Spectra Physics, Tsunami) generating 100 fs pulses with a repetition-rate of 80 MHz, is focalized on the sample with a microscope objective (Olympus, SLMPlan, X20, N. A = 0.35). Samples in powder form are simply deposited onto a microscope slide. The SHG intensity at 450 nm is collected in reflection with the same objective and is separated from the excitation wavelength by a dichroic mirror. The signal is then directed to a spectrometer (Acton research SP2300) coupled with a CCD camera (Princeton Instruments PIXIS 400) via an optical fiber. For each spectrum, the power of the excitation beam is set to 50 mW at the entrance of the microscope and the SHG signal is integrated for 1 second.

Preparation of samples for ferroelectric measurements. **$[Gd_2(L^*)_2(ox)_2(H_2O)_2]$, $[Dy_2(L^*)_2(ox)_2(H_2O)_2]$** are dispersed in epoxy resin (2S epoxy resin from PERSI). This resin is hardened very slowly while adding the catalyst in a vacuum device to avoid both bubbles formation and the degradation of the title compounds. From this treatment, a cylinder shaped block of 0.1 cm length is obtained, which is cut to form a truncated pyramid leading to a rectangle shaped piece of 1 mm length showing two faces parallel to the knife edge. The obtained block is then fixed in a holder and is placed on a vibration proof platform. Slices of resin incorporating the different compounds are then realized with a Reichert-Jung ultra-cut ultra-microtome (thickness of 0.5 μm and motorized cutting stroke of 1 mm/sec). The knife is made from diamond with a 45° angle. The slices are recuperated on water surface and deposited on the fixed copper electrode of the ferroelectric device (Figure S9). The final thickness of the sample film obtained by successive deposition of slices is around 1 μm.

Ferroelectric Measurements. The ferroelectric properties of the system were probed at room temperature using a commercial ferroelectric tester (aixACCT TF 2000E system). It consists in an electrically insulating chamber containing two copper electrodes connected to the ferroelectric tester by shielded coaxial cables. The sample films prepared following the method above were placed between a fixed base electrode, and a mobile top electrode held in place by gravity. The parasitic linear capacitance arising from the ferroelectric tester and the sample fixture was eliminated from the as-measured signal by subtracting the reference signal corresponding to the (linear) parasitic capacitance of the experimental setup (Figure S10). This reference capacitance was measured by placing a thin insulating foil (15 μm-thick optical paper) between the two copper electrodes. The measurement of the I(V) curves is realized at high frequency values of (kHz) in order to minimize leakage current effects.

Magnetic measurements. The magnetic measurements were conducted using a Quantum Design MPMS-3 magnetometer. The static susceptibility measurements were performed in the 1.8 K – 300 K temperature range with an applied field of 0.5 T. Samples were blocked in eicosane to avoid orientation under magnetic field. Magnetization measurements at different fields and at given temperature confirm the absence of ferromagnetic impurities. Data were corrected for the sample holder and eicosane and diamagnetism was estimated from Pascal constants.

Acknowledgements

The authors thank the Centre National de la Recherche Scientifique (CNRS), the Université de Strasbourg (Idex), the Labex NIE (ANR-11-LABX-0058-NIE within the Investissement d'Avenir program ANR-10-IDEX-0002-02), the Agence Nationale de la Recherche (ANR contracts no. ANR-15-CE08-0020-01 and ANR-11-JS10-009-01) and the icFRC (http://www.icfrc.fr) for funding. The authors are grateful to Didier Burger for technical assistance, as well as the SEM platform MEB-Cro and the XRD platform of IPCMS.

Keywords: Ferroelectricity • Coordination polymer • Imidazolium • Rare Earth • Chirality

[[1] M. Lallart, *Ferroelectrics - Applications*, **2011**.
[2] S. Zhang, B. Malič, J.-F. Li, J. Rödel, *J. Mater. Res.* **2021**, *36*, 985–995.
[3] W.-Q. Liao, Y. Zhang, C.-L. Hu, J.-G. Mao, H.-Y. Ye, P.-F. Li, S. D. Huang, R.-G. Xiong, *Nat. Commun.* **2015**, *6*, 7338.
[4] M. Alexe, D. Hesse, *Nat. Commun.* **2011**, *2*, 256.
[5] W. S. Ferreira, *Ferroelectrics* **2023**, *613*, 41–51.
[6] C. Hu, X. Meng, M.-H. Zhang, H. Tian, J. E. Daniels, P. Tan, F. Huang, L. Li, K. Wang, J.-F. Li, Q. Lu, W. Cao, Z. Zhou, *Sci. Adv.* **2020**, *6*, eaay5979.
[7] K. Singh, A. Maignan, C. Martin, Ch. Simon, *Chem. Mater.* **2009**, *21*, 5007–5009.
[8] E. Pachoud, C. Martin, B. Kundys, Ch. Simon, A. Maignan, *J. Solid State Chem.* **2010**, *183*, 344–349.
[9] Y. Saito, H. Takao, T. Tani, T. Nonoyama, K. Takatori, T. Homma, T. Nagaya, M. Nakamura, *Nature* **2004**, *432*, 84–87.
[10] J.-F. Li, K. Wang, B.-P. Zhang, L.-M. Zhang, *J. Am. Ceram. Soc.* **2006**, *89*, 706–709.
[11] J. Tellier, B. Malic, B. Dkhil, D. Jenko, J. Cilensek, M. Kosec, *Solid State Sci.* **2009**, *11*, 320–324.
[12] R. E. Newnham, R. W. Wolfe, J. F. Dorrian, *Mater. Res. Bull.* **1971**, *6*, 1029–1039.
[13] E. C. Subbarao, *J. Phys. Chem. Solids* **1962**, *23*, 665–676.
[14] S. Zhang, N. Kim, T. R. Shrout, M. Kimura, A. Ando, *Solid State Commun.* **2006**, *140*, 154–158.
[15] L. Li, X. Shang, S. Wang, N. Dong, C. Ji, X. Chen, S. Zhao, J. Wang, Z. Sun, M. Hong, J. Luo, *J. Am. Chem. Soc.* **2018**, *140*, 6806–6809.
[16] Y. Ai, R. Sun, W.-Q. Liao, X.-J. Song, Y.-Y. Tang, B.-W. Wang, Z.-M. Wang, S. Gao, R.-G. Xiong, *Angew. Chem. Int. Ed.* **2022**, *61*, e202206034.
[17] D. Khomskii, *Physics* **2009**, *2*.
[18] J. P. Velev, S. S. Jaswal, E. Y. Tsymbal, *Philos. Trans. R. Soc. Math. Phys. Eng. Sci.* **2011**, *369*, 3069–3097.
[19] M. Gajek, M. Bibes, S. Fusil, K. Bouzehouane, J. Fontcuberta, A. Barthelemy, A. Fert, *Nat. Mater.* **2007**, *6*, 296–302.
[20] J. F. Scott, *Nat. Mater.* **2007**, *6*, 256–257.
[21] W. Eerenstein, N. D. Mathur, J. F. Scott, *Nature* **2006**, *442*, 759–765.
[22] N. A. Spaldin, *Proc. R. Soc. Math. Phys. Eng. Sci.* **2020**, *476*, 20190542.
[23] G. Rogez, N. Viart, M. Drillon, *Angew. Chem. Int. Ed.* **2010**, *49*, 1921–1923.
[24] R. Ramesh, *Nature* **2009**, *461*, 1218–1219.
[25] A. K. Cheetham, C. N. R. Rao, *Science* **2007**, *318*, 58–59.
[26] E. Pardo, C. Train, H. Liu, L.-M. Chamoreau, B. Dkhil, K. Boubekeur, F. Lloret, K. Nakatani, H. Tokoro, S. Ohkoshi, M. Verdaguer, *Angew. Chem. Int. Ed.* **2012**, *51*, 8356–8360.
[27] A. O. Polyakov, A. H. Arkenbout, J. Baas, G. R. Blake, A. Meetsma, A. Caretta, P. H. M. van Loosdrecht, T. T. M. Palstra, *Chem. Mater.* **2012**, *24*, 133–139.
[28] B. Kundys, A. Lappas, M. Viret, V. Kapustianyk, V. Rudyk, S. Semak, C. Simon, I. Bakaimi, *Phys. Rev. B* **2010**, *81*, 224434.
[29] H. Tokoro, S. Ohkoshi, *Dalton Trans.* **2011**, *40*, 6825–6833.
[30] S. Ohkoshi, H. Tokoro, T. Matsuda, H. Takahashi, H. Irie, K. Hashimoto, *Angew. Chem. Int. Ed.* **2007**, *46*, 3238–3241.
[31] H. Cui, Z. Wang, K. Takahashi, Y. Okano, H. Kobayashi, A. Kobayashi, *J. Am. Chem. Soc.* **2006**, *128*, 15074–15075.
[32] P. Jain, V. Ramachandran, R. J. Clark, H. D. Zhou, B. H. Toby, N. S. Dalal, H. W. Kroto, A. K. Cheetham, *J. Am. Chem. Soc.* **2009**, *131*, 13625–13627.
[33] M. Sánchez-Andújar, L. C. Gómez-Aguirre, B. Pato Doldán, S. Yáñez-Vilar, R. Artiaga, A. L. Llamas-Saiz, R. S. Manna, F. Schnelle, M. Lang, F. Ritter, A. A. Haghighirad, M. A. Señarís-Rodríguez, *CrystEngComm* **2014**, *16*, 3558–3566.
[34] A. Stroppa, P. Barone, P. Jain, J. M. Perez-Mato, S. Picozzi, *Adv. Mater.* **2013**, *25*, 2284–2290.
[35] T. Besara, P. Jain, N. S. Dalal, P. L. Kuhns, A. P. Reyes, H. W. Kroto, A. K. Cheetham, *Proc. Natl. Acad. Sci.* **2011**, *108*, 6828–6832.
[36] M. Sánchez-Andújar, S. Presedo, S. Yáñez-Vilar, S. Castro-García, J. Shamir, M. A. Señarís-Rodríguez, *Inorg. Chem.* **2010**, *49*, 1510–1516.

[37] G.-C. Xu, X.-M. Ma, L. Zhang, Z.-M. Wang, S. Gao, *J. Am. Chem. Soc.* **2010**, *132*, 9588–9590.
[38] Q. Ye, D.-W. Fu, H. Tian, R.-G. Xiong, P. W. H. Chan, S. D. Huang, *Inorg. Chem.* **2008**, *47*, 772–774.
[39] W. Zhang, R.-G. Xiong, S. D. Huang, *J. Am. Chem. Soc.* **2008**, *130*, 10468–10469.
[40] Q. Ye, T. Hang, D.-W. Fu, G.-H. Xu, R.-G. Xiong, *Cryst. Growth Des.* **2008**, *8*, 3501–3503.
[41] K. Asadi, M. A. van der Veen, *Eur. J. Inorg. Chem.* **2016**, *2016*, 4332–4344.
[42] P. Farger, C. Leuvrey, G. Rogez, M. François, P. Rabu, E. Delahaye, *Cryst. Growth Des.* **2019**, *19*, 4264–4272.
[43] P. Farger, C. Leuvrey, M. Gallart, P. Gilliot, G. Rogez, J. Rocha, D. Ananias, P. Rabu, E. Delahaye, *Beilstein J. Nanotechnol.* **2018**, *9*, 2775–2787.
[44] P. Farger, C. Leuvrey, M. Gallart, P. Gilliot, G. Rogez, P. Rabu, E. Delahaye, *Magnetochemistry* **2017**, *3*, 1–20.
[45] N. P. Martin, C. Falaise, C. Volkringer, N. Henry, P. Farger, C. Falk, E. Delahaye, P. Rabu, T. Loiseau, *Inorg. Chem.* **2016**, *55*, 8697–8705.
[46] T. Ekanayaka, T. Jiang, E. Delahaye, O. Perez, J.-P. Sutter, D. Le, A. T. N'Diaye, R. Streubel, T. S. Rahman, P. A. Dowben, *Phys. Chem. Chem. Phys.* **2023**, *25*, 6416–6423.
[47] A. Dhingra, X. Hu, M. F. Borunda, J. F. Johnson, C. Binek, J. Bird, A. T. N'Diaye, J.-P. Sutter, E. Delahaye, E. D. Switzer, E. del Barco, T. S. Rahman, P. A. Dowben, *J. Phys. Condens. Matter* **2022**, *34*, 441501.
[48] L. Pintilie, M. Alexe, *Appl. Phys. Lett.* **2005**, *87*, 112903.
[49] C. Benelli, D. Gatteschi, *Chem. Rev.* **2002**, *102*, 2369–2388.
[50] O. Kühl, S. Millinghaus, P. Wehage, *Cent. Eur. J. Chem.* **2010**, *8*, 1223–1226.
[51] O. Kühl, G. Palm, *Tetrahedron Asymmetry* **2010**, *21*, 393–397.

10.1002/zaac.202400005

WILEY-VCH

ARTICLE

Entry for the Table of Contents (Please choose one layout)

Layout 1:

FULL PAPER

Text for Table of Contents

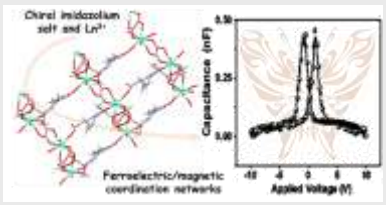

P. Farger, [a] *C. Leuvrey,* [a] *M. Lenertz,* [a] *G. Taupier,* [a, b] *K. D. Dorkenoo,* [a] *D. Ihiawakrim,* [a] *S. Cherifi-Hertel,* [a] *G. Rogez,* [a] *P. Rabu,* [a] *E. Delahaye** [a,c]

Page No. – Page No.

Ferroelectric order in the chiral coordination polymers $[Ln_2(L^*)_2(ox)_2(H_2O)_2]$ with Ln = Gd^{3+} or Dy^{3+}, L* = ((S, S)-1,3-bis(1-carboxylethyl)imidazolium and ox = oxalate.

Layout 2:

FULL PAPER

*Author(s), Corresponding Author(s)**

Page No. – Page No.

Title

Text for Table of Contents

10.1002/zaac.202400005

WILEY-VCH

ARTICLE

Additional Author information for the electronic version of the article.

Author: Emilie Delahaye ORCID identifier 0000-0001-9114-1682
Author: Pierre Rabu ORCID identifier 0000-0002-6779-1527
Author: Guillaume Rogez ORCID identifier 0000-0001-9006-7273
Author: Salia Cherifi-Hertel ORCID identifier 0000-0002-9617-2098
Author: Dris Ihiawakrim ORCID identifier 0000-0002-4410-2768
Author: Marc Lenertz ORCID identifier 0000-0002-6989-9654
Author: Pierre Farger ORCID identifier 0000-0002-5602-3127